Int. J. Heat Mass Transfer. Vol. 25, No. 3, pp. 337–343, 1982
Printed in Great Britain

0017-9310/82/030337–07 $03.00/0
Pergamon Press Ltd.

EFFECTS OF GEOMETRICAL IMPERFECTION AT THE ONSET OF CONVECTION IN A SHALLOW TWO-DIMENSIONAL CAVITY

P. G. DANIELS
Department of Mathematics, The City University, Northampton Square,
London EC1V 0HB, England

(*Received November* 1980)

Abstract—A theoretical study is made of the effect of geometrical imperfections on the formation of weakly nonlinear convection in a shallow two-dimensional cavity uniformly heated from below. If the sidewalls of the cavity are not quite vertical then convective rolls first appear near these walls and subsequently spread inwards to the centre of the cavity as the Rayleigh number is increased. If the horizontal surfaces are not quite parallel then the major effect is a lateral modulation of the rolls due to a combination of the misalignment of the horizontal surfaces and the presence of the sidewalls. As an interesting special case, the solution for a cavity of uniformly sloping base is presented and asymptotic methods are found to provide a remarkably accurate prediction for the critical Rayleigh number as a function of angle of inclination.

NOMENCLATURE

a, b,	constants;
$a_{1,2,3,4}$,	amplitude equation coefficients;
$A_0(X)$,	amplitude function;
$A(X), A_1(X)$,	scaled amplitude functions;
$A_{\tilde{\alpha}}, B_{\tilde{\alpha}}$,	constants;
d,	cavity height;
$f_{\tilde{\alpha}}(z)$	eigenfunctions;
g,	acceleration of gravity;
$G_0(X), G_1(X)$,	lateral variation of horizontal walls;
G	$= G_0 - G_1$
$h(z)$,	vertical variation of vertical walls;
L,	semi aspect ratio of cavity;
n,	direction normal to sidewalls;
p,	non-dimensional pressure;
p_1,	scaled non-dimensional pressure;
R,	Rayleigh number;
R_0,	critical Rayleigh number for infinite layer;
s,	direction along sidewall;
T_0, T_1,	temperatures of lower and upper surfaces (respectively);
u, w,	non-dimensional velocity components;
u_1, w_1,	scaled non-dimensional velocity components,
x, z,	non-dimensional co-ordinates;
X, X_0, X_1,	scaled horizontal co-ordinates.

Greek symbols

α,	error in alignment of horizontal walls;
$\tilde{\alpha}$,	eigenvalues;
$\bar{\alpha}$,	coefficient of thermal expansion;
β,	error in alignment of vertical walls;
γ_0, γ,	constants;
δ_0, δ,	scaled local Rayleigh numbers;
κ,	thermal diffusivity;
λ,	scaled form of β;
ψ,	non-dimensional stream function;
ρ,	density;
σ,	Prandtl number;
θ,	non-dimensional temperature perturbation;
θ_1,	scaled non-dimensional temperature perturbation;
μ,	scaled form of α;
ν,	kinematic viscosity;
$-\chi_n$,	zeros of the Airy function, Ai.

1. INTRODUCTION

ONE OF the difficulties encountered in experimental studies of the heat transport properties of cavity flows, particularly if the apparatus is constructed on a very small scale, is that of ensuring that the cavity walls are of perfect length and alignment. For example, novel features of experimental results obtained by Ahlers [1] are thought to be attributable [2] to small imperfections in geometry involving typical variations of as little as 3% of the height of the cavity. This paper considers the effect of such imperfections or misalignments on the flow in a shallow 2-dim. cavity of semi-aspect ratio L ($\gg 1$) bounded by rigid surfaces and uniformly heated from below. The upper and lower planes are maintained at constant temperatures T_1 and T_0 (respectively) where $T_0 > T_1$, and are assumed to be horizontal to within an error in height of magnitude α. The sidewalls are taken as either perfect insulators or conductors and are assumed to be vertical (i.e. aligned with the direction of gravity) to within an error in inclination of magnitude β. The remaining parameters of the problem are the Rayleigh number R and Prandtl number σ defined by

$$R = \bar{\alpha} g d^3 (T_0 - T_1)/\kappa\nu, \quad \sigma = \nu/\kappa \qquad (1.1)$$

where $\tilde{\alpha}$, κ and ν are respectively the coefficient of thermal expansion, thermal diffusivity and kinematic viscosity of the fluid; d is taken as the vertical height of the cavity at its central point. The steady 2-dim. Oberbeck–Boussinesq equations are then

$$u_x + w_z = 0,$$
$$\sigma^{-1}(uu_x + wu_z) = -p_x + \nabla^2 u,$$
$$\sigma^{-1}(uw_x + ww_z) = -p_z + \nabla^2 w + \theta,$$
$$u\theta_x + w\theta_z = Rw + \nabla^2\theta. \quad (1.2)$$

Here the co-ordinates x, z, velocity components u, w and reduced pressure p are non-dimensional with respect to the quantities $d, \kappa/d$ and $\rho\kappa^2/d^2$ where ρ is the density of the fluid and $\nabla^2 = (\partial^2/\partial x^2) + (\partial^2/\partial z^2)$. θ is the non-dimensional perturbation from the basic linear conductive temperature field:

$$T = T_0 + (T_1 - T_0)z + \left(\frac{\kappa\nu}{\tilde{\alpha}gd^3}\right)\theta. \quad (1.3)$$

The origin of co-ordinates is taken at the centre of the lower surface (see Fig. 1).

Although in a 3-dim. layer of rectangular planform the rolls tend to align with the shorter side (Davis [3]) it should be stressed that this does not imply that the present results are physically unrealistic. Provided the aspect ratio in the third dimension is smaller than $2L$ (but still large compared to 1) we may envisage the present solutions to apply, at least qualitatively, to the region which excludes the immediate neighbourhood of the walls parallel to the x direction. Of course the imperfect geometry may itself affect the alignment of the rolls and in a related study of the effect of a lateral temperature gradient in an infinite system, Weber [4] has shown that rolls aligned perpendicular to the direction of lateral variation, as we assume here, are in fact preferred over a wide range of Prandtl numbers.

2. SIDEWALL MISALIGNMENT

In this section we assume the upper and lower rigid surfaces to be perfectly horizontal so that

$$u = w = \theta = 0 \ (z = 0, z = 1), \quad (2.1)$$

but assume a misalignment of the left-hand sidewall, its position being given by

$$x = -L + \beta h(z), \quad (2.2)$$

where h is an arbitrary function of z and $\beta \ll 1$. If this wall is assumed to be rigid and perfectly insulating we require

$$u(-L + \beta h, z) = w(-L + \beta h, z) = \frac{\partial T}{\partial n}(-L + \beta h, z) = 0, \quad (2.3)$$

where n is the normal direction to the wall. Expansion in Taylor series and use of (1.3) shows that at leading order these boundary conditions become

$$u(-L, z) = w(-L, z) = 0, \quad \frac{\partial \theta}{\partial x}(-L, z) = -\beta R h'(z). \quad (2.4)$$

Clearly the non-zero component of the boundary condition (2.4) will generate motion near the sidewall, where $x + L = O(1)$, for all values of the Rayleigh number, this motion being governed by the linear version of equations (1.2), which may be written in the form

$$\nabla^6\psi - R\psi_{xx} = 0, \quad (2.5)$$

where ψ is the stream function defined by $u = \psi_z$, $w = -\psi_x$. The solution near the sidewall may thus be expressed as

$$\psi = \beta \sum_{\substack{\mathrm{Im}(\alpha_1) > 0 \\ \alpha_2 > 0}} \{A_{\alpha_1} e^{i\alpha_1(x+L)} f_{\alpha_1}(z) + A^*_{\alpha_1} e^{-i\alpha_1^*(x+L)} f^*_{\alpha_1}(z) + B_{\alpha_2} e^{-\alpha_2(x+L)} f_{\alpha_2}(z)\}, \quad (2.6)$$

where * denotes complex conjugate and $\tilde{\alpha} = \alpha_1, -\alpha_1^*$ and $i\alpha_2$ are the triply-infinite set of eigenvalues, with corresponding eigenfunctions f_{α_1}, $f^*_{\alpha_1}$ and f_{α_2} of the system

$$\left(\frac{d^2}{dz^2} - \tilde{\alpha}^2\right)^3 f_{\tilde{\alpha}} + R\tilde{\alpha}^2 f_{\tilde{\alpha}} = 0,$$

$$f_{\tilde{\alpha}} = f'_{\tilde{\alpha}} = f^{iv}_{\tilde{\alpha}} - 2\tilde{\alpha}^2 f''_{\tilde{\alpha}} = 0 \quad (z = 0, 1), \quad (2.7)$$

resulting from equation (2.5) and boundary conditions (2.1). The corresponding solution for θ may be determined from $\theta_x = \nabla^4\psi$. The determination of the eigenvalues $\tilde{\alpha}$ with positive imaginary part presents a considerable numerical problem and although the corresponding eigenfunctions $f_{\tilde{\alpha}}$ will not be orthogonal we may, in principle, suppose that they are complete so that the three boundary conditions will determine the values of each set of three real constants comprising B_{α_2} and the real and imaginary parts of A_{α_1}. Of course (2.7) is the classical Bénard problem (see [5]) and when R reaches the critical value of $R_0 = 1707.8$ the imaginary part of the leading eigenvalue, α_1, becomes zero (i.e. $\alpha_1 \to \alpha_0$ with α_0 real) and two components of the solution (2.6) no longer decay into the bulk of the cavity. The entire procedure can be described analytically by replacing the rigid horizontal surfaces by stress-free ones, since then the $f_{\tilde{\alpha}}$ are orthogonal, $f_{\tilde{\alpha}} = \sin n\pi z$, ($n = 1, 2 \ldots$), $R_0 = 27\pi^4/4$, $\alpha_0 = \pi/\sqrt{2}$ and the A_{α_1} and B_{α_2} can be determined explicitly from (2.4) by Fourier decomposition of $h'(z)$.

When R just exceeds R_0 the motion in the bulk of the cavity can be described using a multiple scales approach. It is convenient to expand the solution using L^{-1} as a single small parameter (see [6]) and then significant changes in the cellular motion first occur in the range

$$R = R_0 + \delta_0 L^{-2}, \quad (2.8)$$

where $\delta_0 = O(1)$. The solution in the bulk has the form

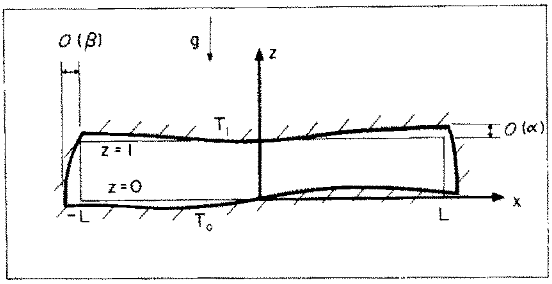

FIG. 1. Schematic diagram of the cavity cross-section.

$$\psi = L^{-1}\{A_0(X)e^{i\alpha_0 x} + A_0^*(X)e^{-i\alpha_0 x}\}f_{\alpha_0}(z) + O(L^{-2}), \quad (-1<X<1), \quad (2.9)$$

where $X = L^{-1}x$ and f_{α_0} is the real eigenfunction corresponding to α_0. The expansion is continued to terms of $O(L^{-3})$ to determine the compatibility equation for the amplitude function A_0, which has the form

$$A_{0_{XX}} + a_1\delta_0 A_0 - (a_2 + \sigma^{-1}a_3)A_0|A_0|^2 = 0 \quad (2.10)$$

where a_1, a_2 and a_3 are positive numerical constants which have been determined previously (see for example [7]). In the stress-free case their values may be determined analytically as $a_1 = 1/18\pi^2, a_2 = \pi^2/16, a_3 = 0$. The boundary condition for this equation at $X = -1$ is given by matching the bulk solution (2.9) to the sidewall solution (2.6) which requires that $\beta A_{\alpha_0}e^{i\alpha_0 L} = L^{-1}A_0(-1)$. Thus in the critical range of Rayleigh number given by (2.8) the misalignment of a perfectly insulating sidewall has a significant effect on the motion throughout the container if $\beta = O(L^{-1})$, and if the sidewall at $x = L$ has a similar misalignment then equation (2.10) must be solved subject to boundary conditions of the form

$$A_0(-1) = (\beta L)ae^{i\gamma}, \quad A_0(1) = (\beta L)be^{-i\gamma}, \quad (2.11)$$

where $\gamma = \alpha_0 L + \gamma_0$ and a, b and γ_0 are numerical constants. In the stress-free case a is given by $a = 3\int_0^1 h'\sin \pi z\, dz$, with $\gamma_0 = \cot^{-1}(1/2\sqrt{2})$.

If the sidewalls are perfect conductors the third boundary condition in (2.3) is replaced by

$$T(-L + \beta h, z) = T_0 + (T_1 - T_0)s/s_{max} \quad (2.12)$$

where s measures distance along the wall. Expansion in Taylor series and use of (1.3) now shows that (2.4) is replaced by

$$u(-L,z) = w(-L,z) = 0,$$
$$\theta(-L,z) = \tfrac{1}{2}\beta^2 R\left[z\int_0^1 h'^2\, dz - \int_0^z h'^2\, dz\right]. \quad (2.13)$$

Thus the misalignment of a perfectly conducting wall has a significant effect if $\beta = O(L^{-1/2})$ and the boundary conditions (2.11) are replaced by conditions of the form

$$A_0(-1) = (\beta^2 L)ae^{i\gamma}, \quad A_0(1) = (\beta^2 L)be^{-i\gamma}. \quad (2.14)$$

Note that in this case the effect disappears if the sidewall slopes at a constant angle since then h' is constant in (2.13) giving $\theta(-L,z) = 0$; the constant a is then zero, as for a vertical wall.

3. LATERAL MISALIGNMENT

Consider now the modifications which occur if the upper and lower surfaces are maintained at constant temperatures T_1 and T_0 but are no longer perfectly horizontal. Let us suppose that the surfaces are given by

$$z = \alpha G_0(X) \text{ and } z = 1 + \alpha G_1(X), \quad (3.1)$$

where we assume initially that $\alpha \ll 1$. The boundary conditions are then

$$u(x,\alpha G_0) = w(x,\alpha G_0) = u(x, 1 + \alpha G_1) = w(x, 1 + \alpha G_1) = 0,$$
$$T(x,\alpha G_0) = T_0, \quad T(x, 1 + \alpha G_1) = T_1, \quad (3.2)$$

and expansion in Taylor series and use of (1.3) yields at leading order

$$u(x,0) = w(x,0) = u(x,1) = w(x,1) = 0,$$
$$\theta(x,0) = \alpha R G_0(X), \quad \theta(x,1) = \alpha R G_1(X). \quad (3.3)$$

The motion generated in the cavity by these boundary conditions can be determined from equations (1.2). In the bulk

$$u = L^{-1}\alpha u_1(X,z) + \ldots, \quad w = L^{-2}\alpha w_1(X,z) + \ldots,$$
$$p = \alpha p_1(X,z) + \ldots, \quad \theta = \alpha\theta_1(X,z) + \ldots \quad (3.4)$$

where

$$u_{1_X} + w_{1_z} = 0, \quad 0 = -p_{1_X} + u_{1_{zz}},$$
$$0 = -p_{1_z} + \theta_1, \quad \theta_{1_{zz}} = 0. \quad (3.5)$$

The appropriate solutions which satisfy the boundary conditions (3.3) are

$$\theta_1 = R[G_0 + (G_1 - G_0)z],$$
$$u_1 = R[\tfrac{1}{24}(G_1' - G_0')z^4 + \tfrac{1}{6}G_0' z^3 - \tfrac{1}{40}(7G_0' + 3G_1')z^2 + \tfrac{1}{60}(3G_0' + 2G_1')z]. \quad (3.6)$$

These do not satisfy the boundary conditions at the sidewalls of the cavity and so generate additional motions in the end-regions, being effectively equivalent to non-zero boundary conditions similar to those of (2.4) and (2.13) above. If the sidewall is vertical and either perfectly insulating or conducting it follows from (3.4) and (3.6) that the magnitude of the motion generated there is $O(\alpha L^{-1})$ and then the amplitude function A_0 must vanish at $X = \pm 1$. However, the equation for A_0 is now modified by additional terms arising from (3.6) which are due to the variation in height of the layer. The effect is equivalent to a 'local' Rayleigh number varying by an amount $O(\alpha)$ and so the appropriate magnitude of α to modify (2.10) when $\delta_0 = O(1)$ is $O(L^{-2})$. The equation becomes

$$A_{0_{XX}} + a_1\delta_0 A_0 - (\alpha L^2)a_4(G_0 - G_1)A_0 - (a_2 + \sigma^{-1}a_3)A_0|A_0|^2 = 0. \quad (3.7)$$

The corresponding equation for a variation of just the lower surface of an infinite layer has been derived previously by Eagles [8] and the value of the positive numerical constant a_4 may be inferred from his results if required. In the infinite layer $(-\infty<X<\infty)$ equation (3.7) generally has both a discrete and continuous spectrum of solutions, depending upon whether the local Rayleigh number at infinity is subcritical or supercritical (see [8]), but in Section 4 below we find that the presence of sidewalls at $X = \pm 1$ not only removes the continuous spectrum, but has a strong influence on the amplitude profiles across the layer.

4. SOLUTIONS OF THE AMPLITUDE EQUATION

We may combine the effects of lateral and sidewall misalignment by writing

$$\alpha = L^{-2}a_4^{-1}\mu,$$
$$\beta = L^{-1}(a_2+\sigma^{-1}a_3)^{-1/2}\lambda \quad \text{(insulating sidewall)}$$
$$\beta = L^{-1/2}(a_2+\sigma^{-1}a_3)^{-1/4}\lambda^{1/2} \quad \text{(conducting sidewall)} \quad (4.1)$$

and with

$$A_0 = (a_2+\sigma^{-1}a_3)^{-1/2}A(X), \quad a_1\delta_0 = \delta, \quad G_0 - G_1 = G(X), \quad (4.2)$$

we obtain from (3.7), (2.11) and (2.14) the general system

$$A_{XX} + \delta A - \mu G(X)A - A|A|^2 = 0, \quad A(-1) = \lambda a e^{i\gamma}, \quad A(1) = \lambda b e^{-i\gamma}. \quad (4.3)$$

Solutions of this system in the case $\mu = 0$ have already been discussed by [6] in the context of imperfectly insulated vertical sidewalls, the parameter λ then representing the magnitude of the heat flow through the sidewalls rather than their slope. The main effect of non-zero λ is to displace the bifurcation of solutions at $\delta = (m\pi/2)^2, (m = 1, 2\ldots)$ for $\lambda = 0$ into solutions in which the amplitude A increases smoothly with Rayleigh number, δ, the value of A being largest initially near the sidewalls so that the convection cells spread inwards from these walls as the Rayleigh number increases. A smooth increase of amplitude of this kind is consistent with the observations of [1].

The situation is modified by a further lateral modulation of the cells if the upper and lower surfaces are sloping, $\delta - \mu G$ then representing an effective local Rayleigh number in equation (4.3). This effect may be seen in isolation by taking $\lambda = 0, G_1 = 0$ and $G_0 = X + 1$ so that the upper surface is horizontal but the lower one slopes upwards from the vertical sidewall at $x = -L$ at an angle $\mu a_4^{-1} L^{-3}$. It emerges that asymptotic solutions of (4.3) yield an extremely accurate prediction of the variation of the critical Rayleigh number over the entire range of angles $0 \leq \mu < \infty$.

First, by formally taking μ small in (4.3) we may perturb about the linear eigensolution $A \propto \cos \pi X/2$ at $\delta = \pi^2/4$ to obtain the critical value of δ at the onset of convection as

$$\delta_c = \frac{\pi^2}{4} + \mu - \left(\frac{5}{\pi^4} - \frac{1}{3\pi^2}\right)\mu^2 + \ldots, \quad (\mu \to 0). \quad (4.4)$$

As δ increases from this value the effect of the inclination of the base, μ, remains small and so the profile of A remains virtually symmetric about the centre of the cavity as the amplitude rises from its initial form near $\delta = \delta_c$:

$$|A| \sim \frac{2}{\sqrt{3}}(\delta-\delta_c)^{1/2}\cos\frac{\pi X}{2}, \quad (\delta \to \delta_c) \quad (4.5)$$

to its limiting uniform distribution

$$|A| \sim \delta^{1/2}, \quad (\delta \to \infty). \quad (4.6)$$

Boundary layers near each sidewall where $1 \pm X = O(\delta^{-1/2})$ and

$$|A| \sim \delta^{1/2}\tanh\left[\left(\frac{\delta}{2}\right)^{1/2}(1 \pm X)\right] \quad (4.7)$$

adjust the solution (4.6) to the sidewall conditions at $X = \mp 1$.

Alternatively, we may take μ large in (4.3) and the flow is then strongly asymmetric. The linear eigensolutions of (4.3) are given by

$$A \propto Ai\{-\mu^{-2/3}[\delta - \mu(X+1)]\}; \quad \delta = \mu^{2/3}\chi_n, \ (\mu \gg 1) \quad (4.8)$$

where Ai is the Airy function whose zeros are denoted by $-\chi_n$, $(n = 0,1\ldots)$ (see [9]). Thus we now obtain

$$\delta_c \sim \mu^{2/3}\chi_0 = 2.3381\,\mu^{2/3}, \quad (\mu \to \infty) \quad (4.9)$$

and as shown in Fig. 2 a combination of the results (4.4), (4.9) provides an accurate estimate of the value of δ_c over the entire range of angles $0 \leq \mu < \infty$. For $\mu \gg 1$

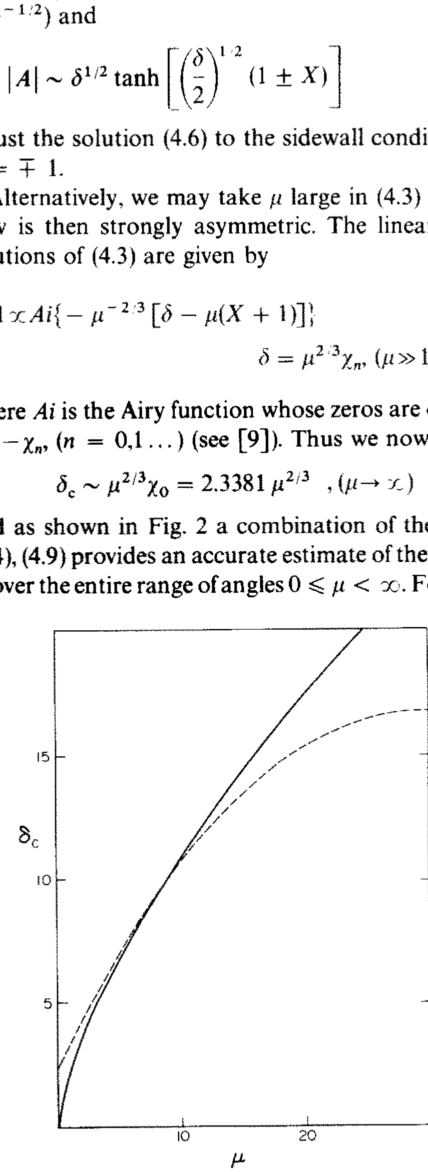

FIG. 2. The local scaled critical Rayleigh number, δ_c, for the onset of convection as a function of the scaled inclination of the base of the cavity, μ, according to the asymptotic formulae (4.4) (dashed lines, strictly valid for $\mu \to 0$) and (4.9) (continuous line, strictly valid for $\mu \to \infty$).

the motion is initially confined to the neighbourhood of the sidewall at $x = -L$, where $X_0 = \mu^{1/3}(X+1) = O(1)$, and

$$|A| \sim \left(\frac{\mu_1}{\mu_2}\right)^{1/2} (\delta - \delta_c)^{1/2} Ai(X_0 - \chi_0) \quad (\delta \to \delta_c). \tag{4.10}$$

Here

$$\mu_1 = \int_0^\infty Ai^2(X_0 - \chi_0)\,\mathrm{d}X_0 = 0.49\ldots,$$
$$\mu_2 = \int_0^\infty Ai^4(X_0 - \chi_0)\,\mathrm{d}X_0 = 0.10\ldots, \tag{4.11}$$

the value of μ_1 having been previously calculated by [10]. As δ increases from δ_c we may expect the convection cells to spread from the sidewall across the cavity, (4.10) eventually developing into the solution

$$|A| \sim [\delta - \mu(X+1)]^{1/2} \quad \left(-1 < X < \frac{\delta}{\mu} - 1\right) \tag{4.12}$$

when $\delta = O(\mu)$. Near the sidewall at $X = -1$ this adjusts to the boundary condition $A(-1) = 0$ through the appropriate solution (4.7) while at $X = \delta/\mu - 1$ there is a region where $X_1 = \mu^{1/3}(1 + X - \delta/\mu) = O(1)$ and $A = \mu^{1/3} A_1(X_1)$. A_1 satisfies the system

$$A_{1_{X_1X_1}} - X_1 A_1 = A_1|A_1|^2,$$
$$|A_1| \sim (-X_1)^{1/2}\ (X_1 \to -\infty), \quad |A_1| \to 0\ (X_1 \to \infty), \tag{4.13}$$

the condition as $X_1 \to -\infty$, ensuring the correct match with (4.12) and that as $X_1 \to \infty$ ensuring the final decay of the convection cells. A relevant numerical solution of (4.13) is described in a different context by the present author [11] and a much wider class of solutions of the real version of the equation, known as the second Painlevé transcendent, has been studied by [12] and [13]. The situation persists until δ reaches the value 2μ; the cells are then in contact with the opposite sidewall ($X = 1$) and an appropriate boundary layer solution, similar to that of (4.7), replaces (4.13). As the Rayleigh number increases the effect of the inclination of the base diminishes and we eventually recover the uniform distribution of convection cells across the cavity, (4.6), as $\delta \to \infty$.

Numerical solutions of the full nonlinear equation at successive values of the scaled Rayleigh number, δ, and at a moderate value of $\mu (= 10)$ are shown in Fig. 3. The nature of the asymmetry is seen to be consistent with the asymptotic analysis above. A quantity of physical relevance, particularly with reference to the measurement techniques in various experimental studies (e.g. [1]) is the heat transfer through the top of the cavity. The two major contributions arising from the instability are a variation on the cellular length scale proportional to $L^{-1}A(X)e^{i\alpha_0 x}$ and a second variation on the scale of the cavity proportional to $L^{-2}|A(X)|^2$, caused by the increment in the mean temperature field. Both contribute to a change in the total heat transfer of $O(L^{-1})$ through the top of the cavity and the effect of the sidewalls and of the slope of the base on the distribution as a function of X can be judged from Fig. 3.

5. DISCUSSION

Imperfections in cavity geometry have been shown to result in two major effects on the pattern of 2-dim. cellular convection that evolves near the critical Rayleigh number. Sloping sidewalls result in the initial development of rolls near the sidewalls and the rolls then spread smoothly inwards as the Rayleigh number increases. Even sloping horizontal surfaces generate a basic flow which is equivalent to a similar non-zero sidewall effect and thus a smooth increase in amplitude but the effect is weak (see Section 3) and will only be significant for Rayleigh numbers closer to the critical value than those considered here. Instead, the main result is a lateral modulation of the rolls, the dominant motion occurring in the vicinity of the largest 'local' Rayleigh number, but then spreading into the rest of the cavity as the Rayleigh number increases. In the range of Rayleigh numbers $R - R_0 = O(L^{-2})$ the sidewall effect is significant for angles of slope $O(L^{-1})$ for perfectly insulating walls and $O(L^{-1/2})$ for perfectly conducting walls (unless the slope is constant in the latter case), while the lateral effect is significant for relatively small angles of slope of the horizontal surfaces of $O(L^{-3})$ and is probably, therefore, one of the major causes for concern in accurate experimental studies of the onset of convection.

It is of interest to note that the analysis of Section 4 shows that for a constant angle of slope $\alpha L^{-1} = L^{-3}a_4^{-1}\mu$ the horizontal extent of the initial region of convection near the sidewall at $x = -L$ is $x + L = O(\mu^{-1/3}L)$ and the solution (2.9) for ψ fails when this is comparable with the width of one convection cell; i.e. $\mu \sim L^3$, when the angle of slope is order one. Of course the basic flow (3.6) throughout the remainder of the cavity is not appropriate when $\alpha = O(1)$ (i.e. $\mu = O(L^2)$) since the Taylor expansions of (3.2) are no longer valid,

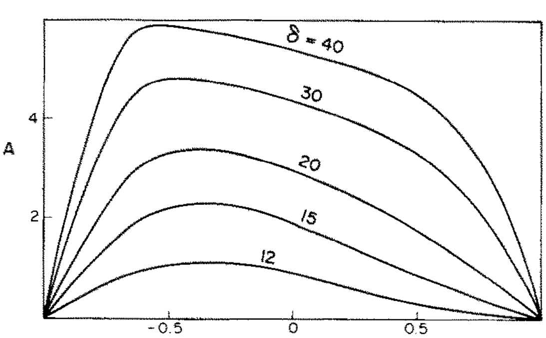

FIG. 3. Profiles of the amplitude of convection across the cavity, $A(X)$, at various values of the scaled Rayleigh number, δ, as determined from (4.3) with $\lambda = 0$, $G_1 = 0$ and $G_0 = X+1$. The scaled angle of inclination of the base is $\mu = 10$.

but with $\alpha \ll L$ this flow remains small, $u = O(\alpha L^{-1})$ and does not change the Airy function solution (4.10) at the onset of convection. In fact the basic state for $\alpha = O(1)$ and general G_0, G_1 can still be found from (3.5) and (3.2) and has

$$\theta_1 = \frac{R[G_0 + (G_1 - G_0)z]}{1 + \alpha(G_1 - G_0)}, \quad (-1 < X < 1), \quad (5.1)$$

in place of (3.6) and u_1 can be found from integration of $u_{1_{zzz}} = \theta_{1_x}$ subject to $u_1\,(X, \alpha G_0) = u_1\,(X, 1+\alpha G_1) = 0$ and the flux constraint $\int_{\alpha G_0}^{1+\alpha G_1} u_1\, dz = 0$.

We have concentrated attention on the range of Rayleigh numbers given by (2.8) since this is the range in which significant changes occur in the amplitude of convection across the cavity. For small values of λ in (4.3) the behaviour of solutions near the onset of convection is also of interest and a series of regimes must be considered as $\lambda \to 0$, and relate to the apparent indeterminacy of the phase of A in (4.3) when $\lambda = 0$. These questions are discussed in detail by Daniels [14]. Other points of interest are the possibility of additional 'phase winding' solutions of (4.3) when $\lambda = O(1)$ (see [15]) although these appear to be limited to higher Rayleigh numbers, $\delta \gg 1$, when λ is small. Also, faster variations in the slope of the horizontal surfaces can have significant effects, particularly if the variations are of a wavelength common with that of the convection (cf. [7]). Finally, we note that if the upper and lower surfaces should be displaced parallel to one another so that $G_0 = G_1$, the extra term in the amplitude equation is no longer present (cf. [4]) and new effects, including a significant interaction between the basic flow and the sidewalls, can arise (Daniels [16]).

REFERENCES

1. G. Ahlers, Low-temperature studies of the Rayleigh–Bénard instability and turbulence, *Phys. Rev. Lett.* **33**, 1185–1188 (1974).
2. R. P. Behringer and G. Ahlers, Heat transport and critical slowing down near the Rayleigh Bénard instability in cylindrical containers, *Phys. Lett.* **62A**, 329–331 (1977).
3. S. H. Davis, Convection in a box: linear theory, *J. Fluid Mech.* **30**, 465–478 (1967).
4. J. E. Weber, On thermal convection between non-uniformly heated planes, *Int. J. Heat Mass Transfer* **16**, 961–970 (1973).
5. S. Chandrasekhar, *Hydrodynamic and Hydromagnetic Stability*, Oxford University Press (1961).
6. P. G. Daniels, The effect of distant sidewalls on the transition to finite amplitude Bénard convection, *Proc. R. Soc.* **A358**, 173–197 (1977).
7. R. E. Kelly and D. Pal, Thermal convection with spatially periodic boundary conditions: resonant wavelength excitation, *J. Fluid Mech.* **86**, 433–456 (1978).
8. P. M. Eagles, A Bénard convection problem with a perturbed lower wall, *Proc. R. Soc.* **A371**, 359–379 (1980).
9. M. Abramowitz and I. A. Stegun, *Handbook of Mathematical Functions*, p. 450. Dover (1964).
10. H. G. Hay, *Phil. Mag. Series* 7, **39**, 928–946 (1948).
11. P. G. Daniels, The effect of centrifugal acceleration on axisymmetric convection in a shallow rotating cylinder or annulus, *J. Fluid Mech.* **99**, 65–84 (1980).
12. J. W. Miles, On the second Painlevé transcendent, *Proc. R. Soc.* **A361**, 277–292 (1978).
13. R. R. Rosales, The similarity solution for the Korteweg–de Vries equation and the related Painlevé transcendent, *Proc. R. Soc.* **A361**, 265–276 (1978).
14. P. G. Daniels, The effect of distant sidewalls on the transition to finite amplitude Bénard convection II, *Mathematika* **25**, 216–235 (1978).
15. M. C. Cross, P. G. Daniels, P. C. Hohenberg and E. D. Siggia, Effect of sidewalls on wavenumber selection in Rayleigh–Bénard convection, *Phys. Rev. Lett.* **45**, 898–901 (1980).
16. P. G. Daniels, The onset of Bénard convection in a shallow sloping container, to appear in *Q. J. Mech. appl. Math.* (1981).

EFFET DE L'IMPERFECTION GEOMETRIQUE SUR LE DEBUT DE CONVECTION DANS UNE CAVITE BIDIMENSIONNELLE ET PEU PROFONDE

Résumé—On étudie théoriquement l'effet des imperfections géométriques sur la formation de la convection faiblement non-linéaire dans une cavité bidimensionnelle peu profonde et uniformément chauffée par le bas. Si les parois latérales de la cavité ne sont pas parfaitement verticales des rouleaux convectifs apparaissent près de ces parois et ils s'étendent vers le centre de la cavité lorsque le nombre de Rayleigh augmente. Si les surfaces horizontales ne sont pas parfaitement parallèles, il en résulte principalement une modulation latérale des rouleaux sous l'effet composé du pincement des surfaces "horizontales" et de la présence des parois latérales. On présente un cas spécial intéressant, la solution pour une cavité avec une base uniformément pentue, et des méthodes asymptotiques fournissant une prédiction remarquablement précise du nombre de Rayleigh critique en fonction de l'angle d'inclinaison.

DIE AUSWIRKUNG GEOMETRISCHER STÖRUNGEN AUF DAS EINSETZEN DER KONVEKTION IN EINEM FLACHEN ZWEIDIMENSIONALEN BEHÄLTER

Zusammenfassung—Es wird eine theoretische Studie über den Einfluß geometrischer Störungen auf die Struktur schwacher nichtlinearer Kovektion in einem flachen zweidimensionalen Behälter, der gleichförmig von unten beheizt wird, durchgeführt. Wenn die Seitenwände des Behälters nicht exakt vertikal sind, erscheinen zuerst an diesen Wänden Konvektionswalzen, die sich danach mit zunehmender Rayleigh-Zahl zum Behälterinneren hin ausbreiten. Sind die horizontalen Begrenzungen nicht vollständig parallel, so ist die Hauptauswirkung eine seitliche Beeninflussung der Walzen, bedingt durch das Zusammenwirken der Nichtparallelität der horizontalen Begrenzungen und der Seitenwände. Als interessanter Spezialfall wird die Lösung für einen Behälter mit gleichförmig schrägem Boden und ein Asymptotenverfahren angegeben, das eine bemerkenswert genaue Berechnung der kritischen Rayleigh-Zahl als Funktion des Neigungswinkels gestattet.

ВЛИЯНИЕ ГЕОМЕТРИЧЕСКИХ ДЕФЕКТОВ НА ВОЗНИКНОВЕНИЕ КОНВЕКЦИИ В УЗКОЙ ДВУХМЕРНОЙ ПОЛОСТИ

Аннотация — Проведено теоретическое исследование влияния геометрических дефектов на возникновение слабо нелинейной конвекции в узкой двухмерной равномерно нагреваемой снизу полости. В случае, когда боковые стенки полости не являются строго вертикальными, конвективные валы появляются сначала возле этих стен, а затем, по мере увеличения числа Релея, распространяются к центру полости. Если же горизонтальные поверхности не строго параллельны, то происходит поперечная модуляция валов из-за совместного влияния непараллельности горизонтальных поверхностей и наличия боковых стен. Представлено решение для специального случая, когда основание полости имеет равномерный наклон. Найдено, что асимптотическими методами можно с большой точностью определить зависимость критического числа Релея от угла наклона.